Supplementary Information: An automated sampling workflow for parallel long-term membrane diffusion cell testing

Claire Benstead, Maria Politi, David S. Bergsman, Lilo D. Pozzo

1 Membrane Permeability: Fickian diffusion across a membrane

As noted in the main article, the diffusion coefficients were determined using a derivation of Fick's law for diffusion across a membrane [1]–[4]. This initial derivation assumes that conservation of mass applies to a closed system, i.e. no dye concentration is lost to aliquot extractions. A discussion of the validity of this assumption for a system in which aliquots are extracted can be found in the following section.

Table 1: Definition of variables.

Variable	**Definition**
A	Area of exposed membrane
C_1	Solute concentration of chamber 1
$C_{1,0}$	Initial solute concentration of chamber 1
C_2	Solute concentration of chamber 2
$C_{2,0}$	Initial solute concentration of chamber 2
C_m	Solute concentration in membrane
D	Diffusion coefficient
J	Flux
L	Membrane thickness
N	total moles of solute in system
P	membrane permeability
t	time
V_{tot}	total solution volume in the system
V_1	volume of solution in donor chamber
V_1^*	volume of donor chamber + 1/2 membrane
V_2	volume of solution in receptor chamber
V_2^*	volume of receptor chamber + 1/2 membrane

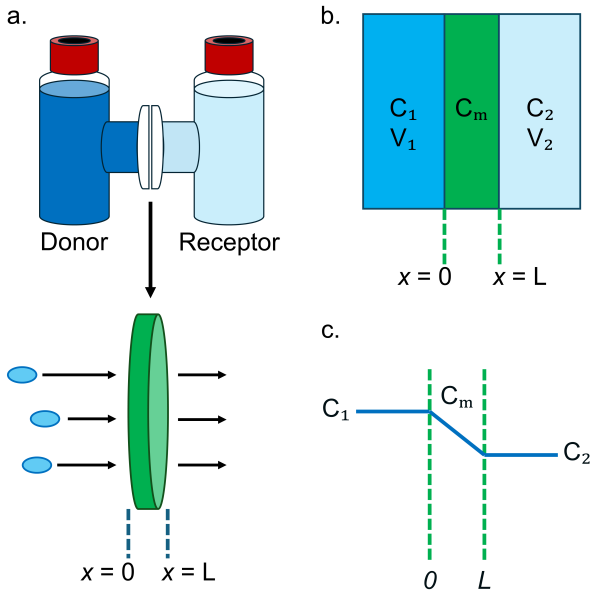

Figure 1: Pseudo-steady state diffusion across a membrane. A) The H-cells used for diffusion testing can be modeled as a donor chamber (C_1) and receptor chamber (C_2) as the dye diffuses across the membrane from $x = 0$ to $x = L$. B) and C) show simplified diagrams for clarity.

1.1 Assumptions

1. The solutions in the H-cells are well-mixed: concentrations at the hydrogel membrane interfaces are equal to bulk solution concentrations.

$$C_1 = C_m(x = 0)$$

$$C_2 = C_m(x = L)$$

2. The concentration profile across the membrane is linear (Fick's first law).
3. Pseudo-steady state: diffusive flux is proportional to the concentration gradient.
4. Diffusion is only in the x-direction, perpendicular to the membrane (no radial diffusion).
5. Diffusion coefficient is independent of concentration.
6. Conservation of mass applies to a closed system: net molar velocity = 0.

Boundary Conditions

$$C_m = C_1 \; at \; x = 0 \; \textbf{(1)}$$

$$C_m = C_2 \; at \; x = L \; \textbf{(2)}$$

$$N = C_{1,0}V_1 \; \textbf{(3)}$$

Initial Conditions

$$t_0 = 0 \; \textbf{(4)}$$

$$C_{m,0} = C_{1,0} \; at \; x = 0 \; \textbf{(5)}$$

$$C_{m,0} = C_{2,0} \; at \; x = L \; \textbf{(6)}$$

1.2 Derivation

From the assumptions stated above and **BCs (1)** and **(2)**, we can define C_m at any point in the membrane (x/L) as

$$C_m = C_1 + (C_2 - C_1)\frac{x}{L} \tag{1}$$

And flux, according to Fick's law:

$$J = -D\frac{dC}{dx} = -D(\frac{C_2 - C_1}{L}) \tag{2}$$

For diffusion in a closed system, conservation of mass applies. The total amount of solute in the system, N, can then be defined as the summation of concentrations in all components:

$$N = C_1V_1 + C_2V_2 + A\int_0^L C_m dx \tag{3}$$

Here, C_m can be substituted with Eq. 1, then integrated and simplified.

$$N = C_1V_1 + C_2V_2 + A\left[C_1L + (C_2 - C_1)\frac{L}{2}\right]$$

$$N = C_1V_1 + C_2V_2 + A\left[\frac{C_1L}{2} + \frac{C_2L}{2}\right]$$

$$N = C_1\left(V_1 + \frac{AL}{2}\right) + C_2\left(V_2 + \frac{AL}{2}\right) \tag{4}$$

Assuming no accumulation and no net molar velocity (no dye is being added or removed from the system), any loss of dye species in the donor chamber is accounted for in the receptor chamber:

$$\frac{dN}{dt} = 0 = \frac{dC_1}{dt}\left(V_1 + \frac{AL}{2}\right) + \frac{dC_2}{dt}\left(V_2 + \frac{AL}{2}\right) \tag{5}$$

The molar velocity of the dye species across the membrane can then be defined using the flux across the membrane (diffusion occurs only in the x-direction, perpendicular to the membrane):

$$JA = \frac{dC_2}{dt}\left(V_2 + \frac{AL}{2}\right) \tag{6}$$

Combining Eq. 2 + 4 + 6, starting with rearranging Eq. 4 to solve for C_1:

$$C_1 = \frac{N - C_2\left(V_2 + \frac{AL}{2}\right)}{\left(V_1 + \frac{AL}{2}\right)}$$

Setting Eq. 2 and 6 equal to each other:

$$\frac{dC_2}{dt}\left(V_2 + \frac{AL}{2}\right) = JA = DA\left(\frac{C_1 - C_2}{L}\right)$$

And substituting C_1 for the rearranged Eq. 4:

$$\frac{dC_2}{dt}\left(V_2 + \frac{AL}{2}\right) = \frac{DA}{L}\left[\frac{N - C_2\left(V_2 + \frac{AL}{2}\right)}{\left(V_1 + \frac{AL}{2}\right)} - C_2\right]$$

$$\frac{dC_2}{dt}\left(V_2+\frac{AL}{2}\right)=\frac{DA}{L}\left[\frac{N-C_2\left(V_2+\frac{AL}{2}\right)}{\left(V_1+\frac{AL}{2}\right)}-\frac{C_2\left(V_1+\frac{AL}{2}\right)}{\left(V_1+\frac{AL}{2}\right)}\right]$$

$$\frac{dC_2}{dt}\left(V_2+\frac{AL}{2}\right)=\frac{DA}{L}\left[\frac{N-C_2(V_1+V_2+AL)}{\left(V_1+\frac{AL}{2}\right)}\right]$$

where $V_{tot}=V_1+V_2+AL$

$$\frac{dC_2}{dt}\left(V_2+\frac{AL}{2}\right)=\frac{DA}{L\left(V_1+\frac{AL}{2}\right)}[N-C_2V_{tot}]$$

$$\frac{dC_2}{dt}\left(V_2+\frac{AL}{2}\right)=\frac{DAV_{tot}}{L\left(V_1+\frac{AL}{2}\right)}\left[\frac{N}{V_{tot}}-C_2\right] \tag{7}$$

To simplify, substitute the volume terms as

$$V_1^*=V_1+\frac{AL}{2}$$

$$V_2^*=V_2+\frac{AL}{2}$$

Assuming the volumes of each chamber of the H-cell are equivalent, $V_1^*=V_2^*$, so

$$V_{tot}=2V_1^*$$

Substituting in the new volume terms to Eq. 7:

$$\frac{dC_2}{dt}=\frac{DAV_{tot}}{LV_1^*V_2^*}\left[\frac{N}{V_{tot}}-C_2\right]$$

$$\frac{dC_2}{dt}=\frac{DAV_{tot}}{L(\frac{1}{2}V_{tot})^2}\left[\frac{N}{V_{tot}}-C_2\right]$$

$$\frac{dC_2}{dt}=\frac{4AD}{LV_{tot}}\left[\frac{N}{V_{tot}}-C_2\right]$$

To simplify for integration, define τ as:

$$\tau=\frac{V_{tot}}{4A}$$

and substitute in:

$$\frac{dC_2}{dt}=\frac{1}{\tau}\frac{D}{L}\left[\frac{N}{V_{tot}}-C_2\right] \tag{8}$$

Integrating Eq. 8 and applying **IC**s:

$$\frac{dC_2}{dt}\frac{1}{\left[\frac{N}{V_{tot}}-C_2\right]}=\frac{D}{L\tau}$$

$$\int\frac{1}{\left[\frac{N}{V_{tot}}-C_2\right]}dC_2\ =\frac{D}{L\tau}\int dt$$

$$-ln\left(\frac{\left(\frac{N}{V_{tot}}\right)_t-C_{2,t}}{\left(\frac{N}{V_{tot}}\right)_{t=0}-C_{2,0}}\right)=\frac{D}{L\tau}t$$

$$-ln\left(\frac{\left(\frac{N}{V_{tot}}\right)_t-C_{2,t}}{\left(\frac{N}{V_{tot}}\right)_{t=0}}\right)=\frac{D}{L}\frac{4A}{V_{tot}}t \tag{9}$$

With conservation of mass, $\left(\frac{N}{V_{tot}}\right)_t=\left(\frac{N}{V_{tot}}\right)_{t=0}$

To solve for the diffusion coefficient using **BC (3)**:

$$N=C_{1,0}\left(V_1+\frac{AL}{2}\right)+C_{2,0}\left(V_2+\frac{AL}{2}\right)$$

$$N=C_{1,0}\left(V_1+\frac{AL}{2}\right)=C_{1,0}V_1^*=C_{1,0}\left(\frac{1}{2}V_{tot}\right)$$

$$-ln\left(\frac{\left(\frac{N}{V_{tot}}\right)_t}{\left(\frac{N}{V_{tot}}\right)_{t=0}}-\frac{C_{2,t}}{\left(\frac{N}{V_{tot}}\right)_{t=0}}\right)=D\frac{4At}{LV_{tot}}$$

$$-ln\left(1-\frac{C_{2,t}}{C_{1,0}\frac{(\frac{1}{2}V_{tot})}{V_{tot}}}\right)=D\frac{4At}{LV_{tot}}$$

$$-ln\left(1-\frac{2C_2}{C_0}\right)=D\frac{4At}{LV_{tot}}$$

The final equation can be written as either form below. Here, V_{tot}, L, A, and C_0 values are obtained experimentally and held constant throughout the length of the experiment.

$$D=-\frac{V_{tot}L}{4At}ln\left(1-\frac{2C_2}{C_0}\right) \tag{10}$$

$$C_2(t)=\frac{C_0}{2}\left[1-e^{-\frac{4AtD}{LV}}\right] \tag{11}$$

Table 2: Variables used for loss of species concentration analysis.

	Term	Defintion
Variable	N	Moles of solute
	C	Concentration of solute
	V	Solution volume
Subscript 1	1	Donor Chamber
	2	Receptor Chamber
	tot	The entire H-cell
	s	sample aliquot
Subscript 2	0	at time $t = 0$
	n	After sampling iteration n is complete
	n-1	After the previous iteration is complete
	nb	Immediately before sampling iteration n begins
	n^*	pertaining to the solute concentration of the sample aliquot of iteration n, equivalent to solute concentration in the H-cell chamber at the time of aliquot extraction, but before the water replenishment step
Superscripts	+	indicates an ideal, closed system

1.3 Impact of Aliquot Extraction on Total Concentration

As described in the main paper, the experimental parameters were designed as to minimize the impact of successive aliquot extractions on total dye concentrations in the H-cells. In other cases where sample aliquots were only extracted from the receptor chamber, the change in volume and/or concentration needed to be accounted for in the approximation [1], [3]. However, since the diffusion coefficient is dependent on the concentration gradient (Eq. 10) rather than species concentration itself, extracting aliquots of equal volume from both chambers and replenishing the volumes lost with water negates the need to account for this extraction in the approximation. As long as the V_{tot} stays constant throughout the experiment, D should not be affected by the slight dilutions induced by each iteration of aliquot extraction and water replenishment.

To understand the impact of successive sampling iterations throughout an experiment on overall species concentration, we can evaluate the loss of species using the following approach. The total number of moles of solute in the H-cells at any given time can be defined as N_n, where n represents the number of sampling iterations completed:

$$N_0 = C_{1,0}V_1 + C_{2,0}V_2$$

$$N_n = C_{1,n}V_1 + C_{2,n}V_2$$

The amount of analyte lost during the sampling iteration, N_{loss}, is equivalent to the amount collected in the aliquots from each chamber:

$$N_{loss} = C_{1,n^*}V_s + C_{2,n^*}V_s$$

Where C_{1,n^*} and C_{2,n^*} are the concentrations of the aliquots from the donor and receptor chambers, respectively, obtained through UV-Vis. Similarly, since C_{1,n^*} and C_{2,n^*} represent the concentrations of the two chambers immediately before iteration n begins, the total amount of solute present in the system prior iteration n can be described as:

$$N_{n-1} = C_{1,n^*}V_1 + C_{2,n^*}V_2$$

To determine the fraction of solute remaining after a sampling iteration:

$$\frac{N_n}{N_{n-1}} = \frac{N_{n-1} - N_{loss}}{N_{n-1}} = 1 - \frac{N_{loss}}{N_{n-1}}$$

Substituting N terms for concentrations, as concentration is the measured value from UV-Vis:

$$1 - \frac{N_{loss}}{N_{n-1}} = 1 - \frac{C_{1,n^*}V_s + C_{2,n^*}V_s}{C_{1,n^*}V_1 + C_{2,n^*}V_2}$$

Since $V_1 = V_2$ and $V_1 + V_2 = V_{tot}$:

$$1 - \frac{V_s(C_{1,n^*} + C_{2,n^*})}{\frac{1}{2}V_{tot}(C_{1,n^*} + C_{2,n^*})} = 1 - \frac{2V_s}{V_{tot}}$$

Therefore, the total amount of solute in the system after a sampling iteration is a given fraction of the amount present prior to the iteration:

$$N_n = N_{n-1}\left[1 - \frac{2V_s}{V_{tot}}\right] \tag{12}$$

Starting with the initial N_0, the N_n after any given sampling iteration can be defined as:

$$N_n = N_0\left[1 - \frac{2V_s}{V_{tot}}\right]^n \tag{13}$$

Following this, the overall loss (%) of species after n successive iterations would be

$$\%\ loss = \frac{N_0 - N_n}{N_0} * 100 = \left(1 - \frac{N_n}{N_0}\right) * 100$$

$$\%\ loss = 1 - \frac{N_0\left[1 - \frac{2V_s}{V_{tot}}\right]^n}{N_0} * 100$$

$$\%\ loss = 1 - \left[1 - \frac{2V_s}{V_{tot}}\right]^n * 100 \tag{14}$$

Figure 2a provides examples of the cumulative loss of species concentration in the H-cells after each successive sampling iteration. For the most impacted set of parameters–a 22 mL H-cell with 20 μL aliquot extractions per chamber–a full 24 iterations of sampling results in an overall species loss of 4.27%. However, since the aliquots are being extracted and replaced from both chambers equally, the overall concentration ratio of the receptor chamber to total concentration (C_2/C_{tot}) does not get significantly affected by this loss.

Within a single sampling iteration, the concentrations of each chamber are reduced by the same factor. In the ideal model described in the assumptions and derivation above (Section 1.2, at any given time t,

$$\frac{2C_2(t)}{C_0} = \frac{2N_2(t)}{V_{tot}}\frac{V_{tot}}{N_0} = \frac{2N_2(t)}{N_0}$$

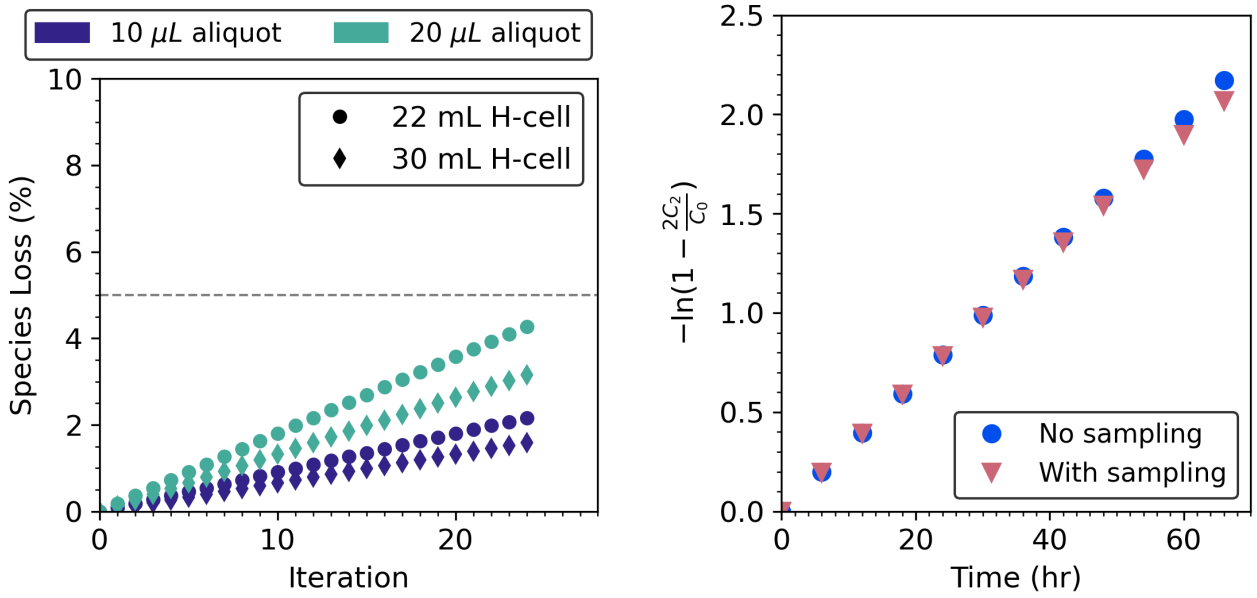

(a) Percentage of dye species lost after successive sampling iterations, for H-cells of 22 or 30 mL total capacity.

(b) $ln(1-\frac{2C_2}{C_0})$ vs t for a hypothetical diffusion test that experiences no species loss (no sampling) compared to successive sample extractions (with sampling).

Figure 2: Impact of aliquot extraction on species loss and diffusion modeling.

where $N_2(t)$ is the amount of solute in the receptor chamber at any given time t. Since the initial concentration ($\frac{1}{2}C_0$) is no longer a constant here, N_0 can instead be substituted with N_n to represent the total amount of solute in the system after a sampling iteration, with N_{n-1} representing total amount of solute prior to the sampling iteration. Alternatively, since $N_2(t)$ is a both a function of time and subject to species loss due to sampling whereas total N is only affected by sampling extraction, $N_{2,nb}$ and $N_{2,n}$ can be used to represent species present in the receptor chamber immediately before and after sampling iteration n. The effect of a sampling iteration on the ratio can then be defined as:

$$\frac{2N_{2,n}}{N_n} = \frac{2N_{2,nb}}{N_{n-1}} \frac{[1-\frac{2V_s}{V_{tot}}]}{[1-\frac{2V_s}{V_{tot}}]} \tag{15}$$

Where $N_{2,nb}$ and N_{n-1} are determined by the concentrations measured with UV-Vis during that iteration (C_{2,n^*} and $C_{1,n^*}+C_{2,n^*}$, respectively).

$$\frac{2N_{2,nb}}{N_{n-1}} = \frac{2C_{2,n^*}V_2}{(C_{1,n^*}+C_{2,n^*})V_2}$$

Therefore, the ratio between concentration in the receptor chamber to the total concentration in the H-cells remains unaffected by the dilution that occurs during a sampling iteration:

$$\frac{2C_{2,n}}{C_{1,n}+C_{2,n}} = \frac{2C_{2,n^*}}{C_{1,n^*}+C_{2,n^*}} \tag{16}$$

Since the ratio before and after a sampling iteration has been completed stays the same, and diffusion is independent

Table 3: Parameters from an AO-through-PES diffusion test.

	Value
Volume (mL)	22
Length (cm)	0.0120
Area (cm^2)	$\pi(0.8)^2$
D ($\times 10^{-7}$ cm^2/s)	3
C_0 (μM)	800
V_s (mL)	0.020
Sample iterations	12
Sample frequency (hrs)	6

of concentration, each sampling iteration has negligible effect
on the actual diffusivity. Any impact on measured diffusivity, then, would be due to the use of C_0 as a constant (unaffected by dilutions, given the assumption of conservation of mass) representing C_{tot} in Eq. 10, whereas the $C_2(t)$ is affected by dilutions.

To understand the effect of holding C_0 constant in overall calculations, we can compare an "ideal" diffusion test in which no sampling, and therefore no species loss, occurs, to one with sampling. Using a hypothetical diffusivity of $3 \times 10^{-7}\ cm^2/s$, along with the parameters listed in Table 3, Eq. 11 can first be used to calculate the hypothetical $C_2^+(t)$ concentration at each iteration time t, assuming complete conservation of mass. This can be used to establish how much the C_2 concentration would change in the time between iteration $n-1$ and n if the system remained undisturbed. $C_{2,n}$ can then be calculated at each sampling time as a function of the chamber concentration after the previous sampling iteration ($C_{2,n-1}$) and the change in receptor chamber concentration of the ideal system within the same time span ($C_{2,n}^+ - C_{2,n-1}^+$) :

$$C_{2,n} = [C_{2,n-1} + (C_{2,n}^+ - C_{2,n-1}^+)] \times [1 - \frac{2V_s}{V_{tot}}] \tag{17}$$

Figure 2b depicts the $ln(1-\frac{2C_2(t)}{C_0})$ term of Eq. 10 vs time for the ideal situation ("No Sampling") and the real situation ("With Sampling"). Although the effect of species loss becomes more apparent as the system approaches equilibrium (i.e., as $ln(1-\frac{2C_2}{C_0})$ approaches $ln(0)$), the calculated diffusivity using the "real" $C_{2,n}$ values, or D_{app}, is $2.945 \pm 0.046 \times 10^{-7}\ cm^2/s$, resulting in a 1.8% error in comparison to a completely ideal situation.

1.4 Effect of Evaporation on Sample Plates

As described in the main paper, the samples prepared by the robot were stored in 96-well polystyrene well plates and characterized using UV-Vis spectroscopy. Pre-slit plate seals were added to reduce water evaporation from the wells in the time between sample collection and characterization. To better understand the impact evaporation might have on data collection and analysis, a well plate was prepared by dispensing 200 μL of 40 μM Acid Orange (AO) to each well. The plate was sealed with a pre-slit film and stored in an OT2 platform for 44 hours, or the typical length of an automated diffusion test. Calibration curves were prepared of the AO solution in an identical well plate for both 200 and 100 μL volumes. UV-Vis of the test plate was collected at the onset of the experiment, after 24 hours of storage, and after 44 hours of storage. 100 μL aliquots of each sample well were then transferred to a new well plate and characterized with UV-Vis.

The final volume in each well was determined using the concentrations of the test plate at time 0 and the 100 μL plate at 44 hours:

$$V_2 = \frac{C_1 V_1}{C_2} \tag{18}$$

In which the volume of solution remaining in each well (V_2) is equal to the original AO concentration (C_1), the initial sample volume (200 μL), and the resulting concentration (C_2), as determined from the 100 μL aliquots. The percentage of volume lost, then, was

$$\%\ loss = \frac{V_1 - V_2}{V_1} * 100$$

The average % volume loss to evaporation over 44 hours was $29.4 \pm 3.1\%$. Although this is a significant change in volume, it should be noted that this does not necessarily affect concentration calculations throughout the length of an automated diffusion experiment. Using the UV-Vis data collected from the original test plate at 0, 24, and 44 hours, AO concentrations were calculated at

each measurement time using the same calibration curve prepared for 200 μL samples, regardless of actual sample volume at that time. After 24 hours–the maximum amount of time samples might be stored between rounds of UV-Vis collection–the concentrations of the samples in the test plate changed by an average of $0.29 \pm 0.36\%$. After 44 hours, the reported concentrations differed from their time 0 values by an average of $0.38 \pm 0.61\%$. This stability in concentrations relative to sample volume can be attributed to the concurrent decrease in pathlength as volume decreases:

$$A = \varepsilon l C$$

$$A = \varepsilon l \frac{mol}{V} = \frac{\varepsilon l [mol]}{\pi r^2 l} \tag{19}$$

Since the plate reader measures absorbance from top-down over the well, the slope of the calibration curve (absorbance A vs concentration C) accounts for both molar absorptivity ε and pathlength l. When evaporation occurs, the decrease in pathlength is directly countered by the decreasing volume of solution. The well radius, total amount of solute (mol) in the well, and molar absorptivity remain constant, thus the measured absorption remains constant. By using the same εl to calculate concentration throughout the length of the experiment, the pathlength, and therefore volume, is treated as a constant, allowing effects of evaporation to be ignored.

2 Partitioning of Aqueous Dyes in PEGDA Hydrogels

Partitioning tests for Brilliant Blue (BB), Acid Orange II (AO), Rhodamine B (RB), and Methylene Blue (MB) were conducted on 25 wt% PEGDA. Hydrogel formulations were prepared as described in the main article. To crosslink as a bulk gel, each solution was poured into a well of a clear, flat-bottom 6-well plate (Cat. No. 10861-554, VWR International) and irradiated at 395 nm for 5 minutes. Four samples (approx. 8 mm diameter, 2.4 mm height) were punched out of each of the four bulk hydrogels so that each dye was tested on 4 unique hydrogels.

In the initial round of testing, the 25 wt% PEGDA bulk gel samples were tested against the experimental concentrations of each dye (150 μM BB, 800 μM AO, 200 μM RB, and 300 μM MB). The hydrogel samples were submerged in 5 mL of dye solution and allowed to sit for a total of 42 hours. UV-Vis data was collected at the start of the experiment, at 24 hours, and at 42 hours by extracting 20 µL aliquots from each sample and diluting to 200 µL in clear, flat-bottom, 96-well polystyrene plates.

Due to the low adsorption of the BB and AO dyes into the hydrogel samples, a second round of testing was conducted using 25 wt% and 40 wt% gel samples and diluted concentrations of the two anionic dyes (7.5 μM BB and 40 μM AO). The hydrogel samples were again submerged in 5 mL of dye solution and allowed to sit for 45 hours. The results of this second round of testing have been reported here alongside the results for the original RB and MB tests. Partitioning coefficient K was determined as the ratio of dye concentration in the hydrogel to concentration in solution [2], [5]:

$$K = \frac{C_{gel}}{C_{soln}} \tag{20}$$

Where

$$C_{gel} = \frac{m_{solute}}{V_{gel}}$$

$$m_{solute} = [C_0 - C_{eq}][V_{soln}]$$

Table 4: Partitioning coefficients of aqueous dyes after reaching equilibrium in 25 wt% PEGDA (K_{25}) and 40 wt% PEGDA (K_{40})

	Charge	K_{P25}	K_{P40}
BB	-2	0.91 ± 0.23	0.57 ± 0.14
AO	-1	4.38 ± 0.49	4.07 ± 0.96
RB	+/-	33.2 ± 7.9	
MB	+1	22.8 ± 1.8	

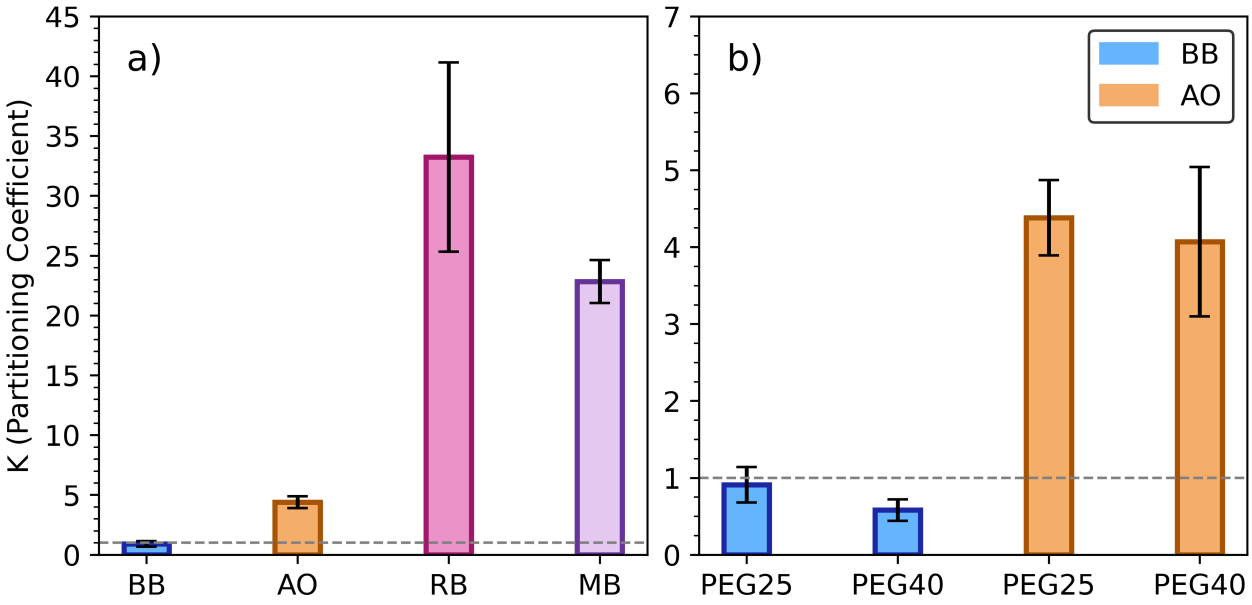

Figure 3: A) Partitioning coefficients of aqueous dyes with 25 wt% PEGDA hydrogels. B) Partitioning of BB and AO for 25 and 40 wt% PEGDA hydrogels.

$$V_{gel} = \frac{\pi}{4} d^2 h$$

$$K = \frac{m_{solute}}{C_{eq} V_{gel}} = \frac{[C_0 - C_{eq}] V_{soln}}{C_{eq} V_{gel}} \tag{21}$$

Where m_{solute} is the amount of dye (in moles), C_{gel} is the concentration of dye in the hydrogel, C_{soln} is the concentration of dye in the aqueous solution, V_{gel} is the volume of the hydrogel sample, and V_{soln} is the volume of the aqueous solution. C_0 is the initial C_{soln}, obtained by UV-Vis at the beginning of the experiment, and C_{eq} is the aqueous dye concentration at equilibrium. A K value of 1 indicates unity, or an equivalent concentration of dye ions within the hydrogel as in the surrounding solution. A value greater than 1 indicates that the dye concentration is higher in the hydrogel sample than in the solution.

As seen in Figure 3, the zwitterionic RB and cationic MB both demonstrated high affinities for the PEGDA hydrogel compared to aqueous solution. For the anionic dyes, the monovalent AO demonstrated a slight preference for the hydrogel, while the divalent BB was largely rejected by the hydrogels. This behavior can be seen in Figure 4. The hydrogel samples, which began clear and colorless, noticeably changed in coloration and opacity after sitting in the dye solutions. The gel sample submerged in the BB solution shows very little uptake of the dye, particularly compared to

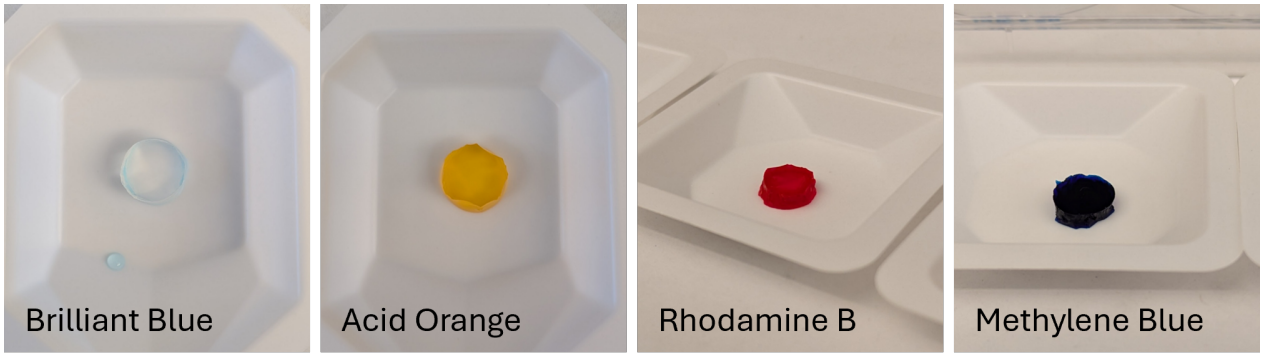

Figure 4: 25 wt% PEGDA hydrogel partitioning samples after reaching equilibrium in their respective dye solutions.

the vivid staining of the RB and MB samples, which were noticeably darker than their respective dye solutions.

2.1 Mass Balance Analysis

The mass balance equation for diffusion across a membrane, accounting for partitioning of the test solute in the membrane:

$$In - Out + Generation = Accumulation$$

With no generation, this simplifies to $In = Out + Accumulation$. Here, the subscript ∞ represents the last sampling iteration collected from the H-cell:

$$C_{1,0}V_1 + C_{2,0}V_2 + C_{gel,0}V_{gel} = C_{1,\infty}V_1 + C_{2,\infty}V_2 + C_{gel,\infty}V_{gel} \tag{22}$$

Since $V_1 = V_2$ and initial $C_{2,0}$ and $C_{gel,0} = 0$:

$$C_{1,0}V_1 = (C_{1,\infty} + C_{2,\infty})V_1 + C_{gel,\infty}V_{gel}$$

Factoring in loss of solute due to sampling (Eq. 13), in which n represents the total number of sampling iterations completed:

$$C_{1,0}V_1\left[1 - \frac{2V_s}{V_{tot}}\right]^n = (C_{1,\infty} + C_{2,\infty})V_1 + C_{gel,\infty}V_{gel} \tag{23}$$

since C_{gel} at equilibrium (or in this case, max time, or ∞) is $= KC_{eq}$ (Eq. 20):

$$C_{gel,\infty} = K\left[\frac{C_{1,\infty} + C_{2,\infty}}{2}\right]$$

$$C_{1,0}V_1\left[1 - \frac{2V_s}{V_{tot}}\right]^n = (C_{1,\infty} + C_{2,\infty})V_1 + \frac{1}{2}K(C_{1,\infty} + C_{2,\infty})V_{gel} \tag{24}$$

Organizing terms:

$$C_{1,0}V_1\left[1 - \frac{2V_s}{V_{tot}}\right]^n = (C_{1,\infty} + C_{2,\infty})(V_1 + \frac{1}{2}KV_{gel}) \tag{25}$$

Where $V_{gel} = \pi r^2 L$.

Table 5: Mass balance analysis of diffusion test samples. Initial and final solution concentrations were determined using the iteration 0 and 11 sample data, with a total of 12 sampling iterations removed from each system.

Dye	Membrane	L (cm)	K	Left (μmol)	Right (μmol)	Δ (μmol)	% Diff
BB	PEG40	0.015	0.57	1.702	1.687	0.015	0.88%
AO	PEG25	0.011	4.38	8.789	8.923	-0.134	1.52%
RB	PEG25	0.014	33.2	2.056	2.020	0.036	1.75%

This mass balance analysis has been performed on three membrane samples, one BB-through-PEG40, one AO-through-PEG25, and one RB-through-PEG25, using the H-cell chamber concentrations at time 0 ($C_{1,0}$ and $C_{2,0}$) and at the end of the experiment ($C_{1,\infty}$ and $C_{2,\infty}$). The left side of the balance, or input, and right side ($out + accumulation$) have been reported in Table 5, along with the difference between the two values ($In - Out - Accum = \Delta$). It should be noted that due to the open nature of the H-cells, chamber volumes may vary from the nominal values used, and can result in a Δ value other than 0 (as seen in Table 5). Dye retention in the membranes may also vary between samples, as seen with the standard deviations present in the measured partitioning coefficients in Table 4. As such, these potential sources of error may affect the mass balance analysis.

3 Delayed Diffusion and Lag Time

In some cases, such as with a test dye that strongly adsorbs to the membrane, initial diffusion is delayed until the membrane has been saturated. By increasing the frequency of automated sampling in the early hours of a permeation test, this delay in diffusion can be observed. Figure 5 demonstrates this behavior, depicting two PEG40 membrane samples tested with RB and AO. AO, which has a relatively low partitioning coefficient compared to RB, experiences a slight delay in diffusion at first, identifiable by the low, non-steady state effective diffusivity at hour 1. The delay for RB, on the other hand, is more noticeable in both the concentration and diffusivity plots, not reaching pseudo-steady state diffusion until about 8 hours after the start of the experiment.

Depending on the materials being tested, the ability to identify and characterize this delay in diffusion using the automated workflow may be highly beneficial, such as for membranes with intentional delays or reactive barrier membranes.[6], [7]

4 Small Angle X-Ray Scattering

Poly(ethylene glycol) diacrylate (PEGDA) hydrogel mesh sizes were determined using small angle x-ray scattering (SAXS). Hydrogel solutions were prepared in clean 5-mL glass vials using deionized water. All samples were prepared with 0.1 wt% lithium phenyl(2,4,6-trimethylbenzoyl) phosphinate (LAP) and deionized water. The formulations were mixed by hand until no visible separation of polymer and aqueous phases could be observed, then were allowed to rest for 30 minutes before crosslinking. To crosslink, each hydrogel formulation was poured into a well of a clear, flat-bottom 6-well plate (Cat. No. 10861-554, VWR International) and irradiated in ambient conditions for 5 minutes with 395 nm light. This resulted in hydrogel samples of approximately 1.3-1.5 mm thickness, depending on the PEGDA concentration. From here, samples were prepared for SAXS by punching out 8-mm diameter cores from the bulk gels using a cork borer.

Samples were then loaded into a 48-sample liquid cartridge stage and SAXS analysis was conducted using a Xenocs Xeuss 3.0 (Xenocs, Grenoble, France) with a copper microfocus X-ray source.

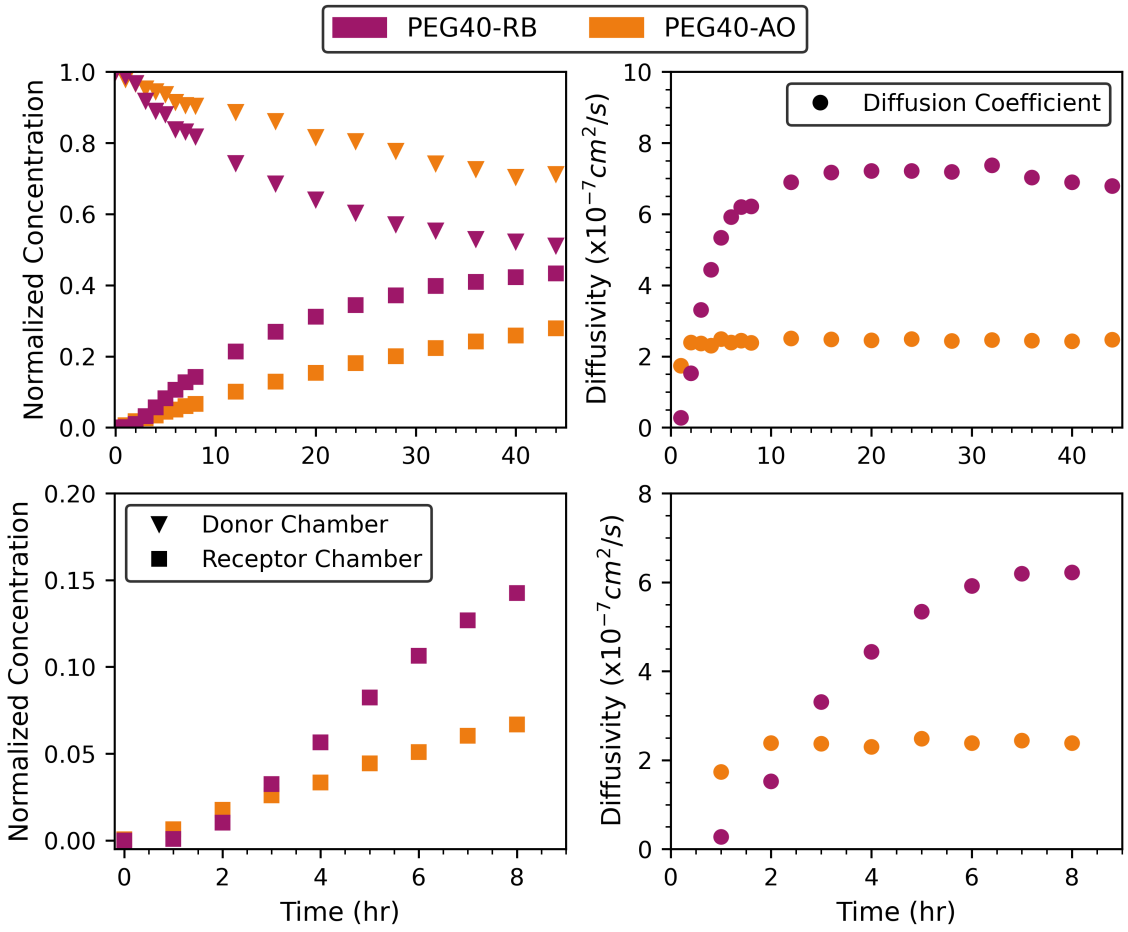

Figure 5: Diffusion of RB and AO through PEG40 membranes. Top: concentration vs time and diffusivity vs time of the full experiment time (44 hours). Bottom: concentration and diffusivity vs time of the first 8 hours.

In total, 4 sample-to-detector distances were used to collect wide-angle and small-angle X-ray scattering (WAXS and SAXS) measurements (0.05 m for 180 s, 0.37 m for 480 s, 0.9 m for 840 s, and 1.8 m for 1140 s). The scattering data collected for each sample were reduced using XSact Software (Xenocs), with a background subtraction of an empty sample position. Determination of hydrogel mesh sizes was completed using the shape-independent broad peak model with the DiffeRential Evolution Adaptive Metropolis (DREAM) algorithm. All model fitting was conducted through the SasView and bumps packages in a Jupyter notebook.

The Broad Peak model, as described in version 5.0.3 of SasView [8]:

$$I(Q) = \frac{A}{q^n} + \frac{C}{1 + (|q - q_0|\xi)^m} + B \tag{26}$$

Here, scattering intensity $I(Q)$ is calculated using the Porod law scaling factor (A), the Porod exponent (n), the Lorentzian scaling factor (C), the exponent of q (m), the screening length (ξ), and the flat background (B). In later versions (i.e., 6.1.0), the additional exponent p is present in the model, however all SAXS data here was fit with the implicit definition of p = 1.[9] It should be noted that screening length and mesh size are generally represented by the same variable (ξ), but are not equivalent. For clarity, mesh size will be represented as ξ_{mesh}. Here, q_0 represents the position of the peak associated with the mesh size, and can be related to d-spacing using the following equations:

$$q = \frac{4\pi sin(\theta)}{\lambda} \tag{27}$$

As described above, q can be defined as a function of the scattering angle (2θ) and wavelength of the Cu-sourced X-rays (λ).

$$\xi_{mesh} = d = \frac{2\pi}{q_o} \tag{28}$$

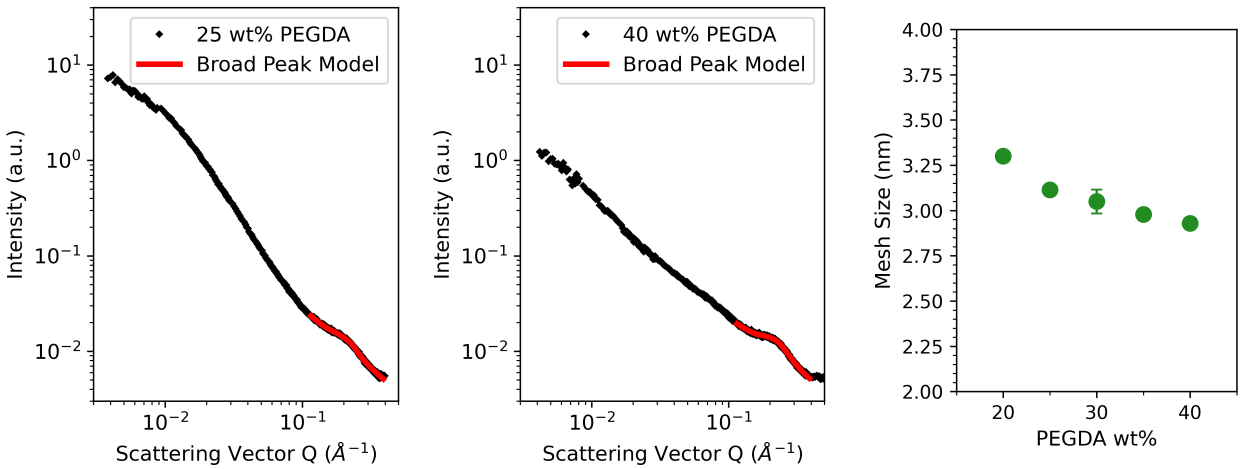

(a) (b) (c)

Figure 6: Sample plots of SAXS results for PEGDA hydrogels. A) and B): example fits of the broad peak model to 25 and 40 wt% PEGDA hydrogels. C) mesh sized of PEGDA hydrogels at varying concentrations of polymer.

For Mn 700 PEGDA hydrogels, the feature (peak/shouldering) that appears at $\sim$ 0.2 A^{-1} is associated with the dominant mesh size of the system. Due to the inherent heterogeneity of

hydrogels that have been crosslinked via radical photopolymerization and scattering interference from larger features, the nominal mesh size represents a distribution of mesh sizes rather than a monodisperse mesh network.

Sample plots of scattering profiles for 25 and 40 wt% PEGDA can be found in Figure 6, along with average mesh sizes determined for these PEGDA hydrogels ranging from 20-40 wt%. The average mesh size was determined using a minimum of 3 samples at each PEGDA wt%. As can be seen in Figure 6C, average mesh sizes range from 2.9-3.3 nm, with an overall decrease in spacing between crosslink junctions as the PEGDA concentration is increased.

References

[1] C. K. Colton, K. A. Smith, E. W. Merrill, and P. C. Farrell, "Permeability studies with cellulosic membranes," en, *Journal of Biomedical Materials Research*, vol. 5, no. 5, pp. 459–488, 1971, ISSN: 1097-4636. DOI: 10.1002/jbm.820050504.

[2] A. Cavallo, M. Madaghiele, U. Masullo, M. G. Lionetto, and A. Sannino, "Photo-crosslinked poly(ethylene glycol) diacrylate (PEGDA) hydrogels from low molecular weight prepolymer: Swelling and permeation studies," en, *Journal of Applied Polymer Science*, vol. 134, no. 2, p. 44 380, 2017, ISSN: 1097-4628. DOI: 10.1002/app.44380.

[3] C. J. Lee, J. A. Vroom, H. A. Fishman, and S. F. Bent, "Determination of human lens capsule permeability and its feasibility as a replacement for Bruch's membrane," *Biomaterials*, vol. 27, no. 8, pp. 1670–1678, Mar. 2006, ISSN: 0142-9612. DOI: 10.1016/j.biomaterials.2005.09.008.

[4] K. Engberg and C. W. Frank, "Protein diffusion in photopolymerized poly(ethylene glycol) hydrogel networks," en, *Biomedical Materials*, vol. 6, no. 5, p. 055 006, Aug. 2011, ISSN: 1748-605X. DOI: 10.1088/1748-6041/6/5/055006.

[5] E. W. Merrill, K. A. Dennison, and C. Sung, "Partitioning and diffusion of solutes in hydrogels of poly(ethylene oxide)," *Biomaterials*, vol. 14, no. 15, pp. 1117–1126, Jan. 1993, ISSN: 0142-9612. DOI: 10.1016/0142-9612(93)90154-T.

[6] R. A. Siegel and E. L. Cussler, "Reactive barrier membranes: Some theoretical observations regarding the time lag and breakthrough curves," *Journal of Membrane Science*, vol. 229, no. 1, pp. 33–41, Feb. 2004, ISSN: 0376-7388. DOI: 10.1016/j.memsci.2003.10.013.

[7] D. Bai, F. Asempour, and B. Kruczek, "Can the time-lag method be used for the characterization of liquid permeation membranes?" *Chemical Engineering Research and Design*, vol. 162, pp. 228–237, Oct. 2020, ISSN: 0263-8762. DOI: 10.1016/j.cherd.2020.08.012.

[8] *Broad_peak SasView 5.0.3 documentation*, Jul. 2016.

[9] *Broad_peak — SasView 6.1.0 documentation*, May 2021.